Dynamics of Axonal Microtubules Regulate the Topology of New Membrane Insertion into the Growing Neurites

Stanislav Zakharenko and Sergey Popov

Department of Physiology and Biophysics, University of Illinois at Chicago, Chicago, Illinois 60612

Abstract. Nerve growth depends on the delivery of cell body–synthesized material to the growing neuronal processes. The cellular mechanisms that determine the topology of new membrane addition to the axon are not known. Here we describe a technique to visualize the transport and sites of exocytosis of cell body–derived vesicles in growing axons. We found that in *Xenopus* embryo neurons in culture, cell body–derived vesicles were rapidly transported all the way down to the growth cone region, where they fused with the plasma membrane. Suppression of microtubule (MT) dynamic instability did not interfere with the delivery of new membrane material to the growth cone region; however, the insertion of vesicles into the plasma membrane was dramatically inhibited. Local disassembly of MTs by focal application of nocodazole to the middle axonal segment resulted in the addition of new membrane at the site of drug application. Our results suggest that the local destabilization of axonal MTs is necessary and sufficient for the delivery of membrane material to specific neuronal sites.

Key words: exocytosis • axon • microtubule • dynamic instability • diffusion

The addition of new membrane to nerve processes is an essential step in nerve growth and differentiation (Craig and Banker, 1994). New membrane components are synthesized in the cell body and delivered to the plasmalemma by fast axonal transport (Allen et al., 1982; Nakata et al., 1998). Inhibition of the new membrane supply, using either pharmacological treatments or the optical tweezers technique, rapidly arrests axonal growth (Martenson et al., 1993; Jareb and Banker, 1997; Chang et al., 1998). The topology of new membrane insertion into the growing nerve processes remains controversial. Insertion of new membrane may occur in the vicinity of the cell body, at the growth cone area, or along the growing neurites (Bray, 1970; Futerman and Banker, 1996). Two different experimental strategies, previously used to determine the sites of new membrane addition to the growing axons, have focused on the different aspects of membrane addition. In the first approach, neurites are tagged with plasma membrane–attached microparticles, or reporter molecules, and movement of these markers is monitored using video microscopy. This method has been designed to detect the sites of bulk membrane insertion into the axon; it does not allow for discrimination between exo- and endocytic contributions to the net addition of the new membrane. The second approach focuses specifically on the exocytic component and attempts to visualize the sites of addition of the newly synthesized plasma membrane proteins or lipids to the plasmalemma.

In the attempts to determine the sites of membrane insertion using the first approach, plasma membrane markers were found to be stationary (Bray, 1970), to move retrogradely (Koda and Partlow, 1976), or to move anterogradely (Zheng et al., 1991; Okabe and Hirokawa, 1992). The translocation of the markers was taken as a measure of the net insertion, or retrieval, of plasma membrane material along the axon proximal to the site of tagging. However, the plasma membrane probes used in these experiments, such as large membrane-associated particles, are likely to be anchored to the axonal cytoskeleton (Abercrombie et al., 1970; Peng and Chang, 1982; Okabe and Hirokawa, 1992; Lin et al., 1996). In this case, the movement of the probes would reflect the translocation of unidentified cytoskeletal elements and may not be related to the movement of plasma membrane lipids, as is the case for nonneuronal translocating cells (Abercrombie et al., 1970; Sheetz et al., 1989; Lee et al., 1990). To overcome this technical limitation, attempts have been made to specifically detect the translocation of plasma membrane lipids (Popov et al., 1993; Dai and Sheetz, 1995). In *Xenopus* spinal cord neurons grown on laminin-coated coverslips, bulk anterograde lipid flow has been reported (Popov et al., 1993), suggesting membrane addition along the neurite. In

Address all correspondence to Sergey Popov, Department of Physiology and Biophysics M/C 901, University of Illinois at Chicago, 835 S. Wolcott Ave., Chicago, IL 60612. Tel.: (312) 413-5682. Fax: (312) 996-1414. E-mail: spopov@uic.edu

contrast, in chick DRG neurons, rapidly diffusing latex microbeads were found to translocate retrogradely (Dai and Sheetz, 1995), indicating preferential membrane addition to the growth cone region and bulk membrane endocytosis at the cell body. The efforts to directly visualize the sites of addition of new proteins or lipid to the growing axon using the second approach have also led to conflicting results (Feldman et al., 1981; Griffin et al., 1981; Pfenninger and Maylie-Pfenninger, 1981; Craig et al., 1995; Harel and Futerman, 1996; Vogt et al., 1996). Thus, strong evidence has been obtained both supporting and opposing the concept of preferential addition of the newly synthesized plasma membrane components to the growth cone region.

In this study, we directly visualized the traffic of new membrane material in the *Xenopus* embryo neurons by locally labeling the cell body–derived vesicles with the fluorescent lipid analogue 1,1′-didodecyl-3,3,3′,3′-tetramethylindocarbocyanide ($DiIC_{12}$).[1] The anterograde transport of new membrane carriers was detected by digital fluorescent microscopy. The new membrane was transported by the cell body–derived tubovesicular organelles, which were delivered to and preferentially inserted into the distal axon. We found that modulation of axonal microtubule dynamics had a dramatic effect on the pattern of membrane addition to the axonal plasmalemma. Thus, the dynamics of axonal microtubules may serve as a basic regulator of the topology of the new membrane addition to the nerve processes.

Materials and Methods

Cell Culture

Xenopus embryo neuronal cultures were prepared as previously reported (Anderson et al., 1977). In brief, the neuronal tube of embryos at stages 19–24 was dissociated in Ca^{2+}- and Mg^{2+}-free solution (115 nM NaCl, 2.6 mM KCl, 10 mM Hepes, 0.4 mM EDTA, pH 7.6). Dissociated cells were plated on glass coverslips precoated with concanavalin A (0.1–1.0 μg/cm^2; Sigma Chemical Co., St. Louis, MO). The cultures were kept at 20°C in culture medium consisting of (vol/vol) 50% Leibovitz L-15 medium (GIBCO BRL; Life Technologies, Gaithersburg, MD), 49% Ringer's solution (115 mM NaCl, 2 mM $CaCl_2$, 2.5 mM KCl, 10 mM Hepes, pH 7.6), 1% fetal bovine serum (GIBCO BRL), and 50 ng/ml neurotrophin-3. The neurons were used for experiments 24–48 h after plating.

Local Labeling of the Cell Body–derived Vesicles

$DiIC_{12}$ (Molecular Probes, Eugene, OR) was prepared as a 1 mg/ml stock solution in methanol. Local perfusion of the cell body was performed according to previously reported methods (Popov et al., 1993). In brief, two pipettes were placed opposite to each other at a distance of 20–40 μm from the neuronal surface. The first pipette (inner diameter 2–3 μm) was filled with 10 μg/ml of $DiIC_{12}$, which was dissolved immediately before experiments in the solution containing 57.5 mM NaCl, 60 mM KCl, 2 mM $CaCl_2$, and 10 mM Hepes, pH 7.6. A small hydrostatic pressure applied to the pipette resulted in a constant outflow of the intrapipette solution. The second pipette with tip opening of ~10 μm was used for removal of the superfusion solution from the culture medium, thereby reducing the affected area to ~30 μm. The pipettes were withdrawn from the soma 30–60 s after the onset of perfusion.

Image Acquisition and Data Analysis

Cells were observed using an inverted microscope (model IX 50; Olympus America, Inc., Melville, NY) equipped with differential interference contrast optics, a 60× Fluorite objective (NA 1.2), and a 100-W mercury lamp. The light passed through an infrared-blocking filter, neutral density filters, and a rhodamine wide-band filter. Images were acquired with a charge-coupled device (CCD) camera (model ImagePoint or SenSys; Photometrics, Tucson, AZ) driven by IPLab (Signal Analytics Corp., Vienna, VA) imaging software. Exposure time was 0.2–1 s. Images were processed with IPLab and Photoshop (Adobe Systems, Mountain View, CA). Quantitation of data was performed using IPLab software. Typically, the distribution of fluorescence intensity along the axon was obtained by measuring the intensity within individual pixels along the length of neurite or along individual filopodia. The background fluorescence, measured in cell-free areas ~10 μm from the axon, was subtracted from the fluorescence at the neurite.

Microinjection of Cy3-tubulin into Xenopus Embryos

Cy3-tubulin was a generous gift of Dr. Gary Borisy (University of Wisconsin, Madison, WI). Details of Cy3-tubulin preparation can be obtained from http://borisy.bocklabs.wisc.edu. *Xenopus* embryos were injected with 10–25 nl of 10 mg/ml Cy3-tubulin as described before (Chang et al., 1998). The embryos were allowed to develop to stages 19–24 and were then used for the preparation of neuronal cultures.

Detergent Extraction

Neurons labeled with Cy3-tubulin were extracted in a microtubule (MT)-stabilizing buffer (60 mM Pipes, 1 mM $MgCl_2$, 5 mM EGTA, 0.1% Triton X-100, 10 μM taxol, pH 6.8) for 5 min and examined under a fluorescent microscope. For each axon, the fluorescence intensity was compared before and after extraction.

Immunocytochemistry

The cells were permeabilized with 0.1% Triton X-100 in solution containing 10 μM taxol, 60 mM Pipes, 1 mM EGTA, 4% polyethylene glycol, and 1 mM $MgCl_2$, pH 6.9, and fixed with 0.5% glutaraldehyde in PBS for 20 min. Glutaraldehyde was quenched with two changes of 2 mg/ml sodium borohydride in PBS. Cells were incubated with a primary and then with a secondary antibody for 1 h at room temperature. All antibody solutions were prepared in PBS containing 2 mg/ml bovine serum albumin. The primary antibody used was a mouse monoclonal antibody to β-tubulin (Amersham Corp., Arlington Heights, IL), and the secondary antibody was rhodamine-conjugated anti–mouse IgG (Jackson ImmunoResearch, West Grove, PA).

Results

Staining of Cell Body–derived Vesicles with Fluorescent Lipid Analogue $DiIC_{12}$

The cultures of *Xenopus* embryo neurons were prepared on a concanavalin A–coated substrate in the presence of the neurotrophic factor neurotrophin-3 (Chang et al., 1998). Under these culture conditions, neurites form ~4–6 h after plating and grow at a the rate of ~30–40 μm/h for a few days; these neurites are usually referred to as "axons" (Reinch et al., 1991; Zheng et al., 1994; Tanaka et al., 1995). Experiments were performed 24–48 h after cell culture preparation on axons that were 1.2–2.0 mm in length and were free of contact with other cells.

We used a local superfusion technique (Popov et al., 1993; Engert and Bonhoeffer, 1997) to stain the plasma membrane at the cell body with fluorescent lipid analogue $DiIC_{12}$ (Fig. 1 *A*). Within 2–3 min after the onset of perfusion, the soma was brightly labeled with $DiIC_{12}$ molecules. Initially, the staining was largely localized to the cell body. With time, plasma membrane staining could be detected at progressively greater distances from the soma (Fig. 1 *B*), consistent with lateral diffusion of $DiIC_{12}$ molecules along

1. *Abbreviations used in this paper:* $DiIC_{12}$, 1,1′-didodecyl-3,3,3′,3′-tetramethylindocarbocyanide; MT, microtubule.

the axonal plasmalemma (Popov et al., 1993). In the first 20 min after cell body labeling, no plasma membrane staining was observed at the distal axonal segment, in agreement with the rapid drop in the rate of diffusional transport with increasing distance. However, fluorescent microscopy of the axon ~1 mm from the soma, well beyond the reach of diffusional transport, revealed brightly stained tubovesicular organelles (Fig. 1 *C*). As judged by the fluorescent microscopy, these organelles ranged from ~0.2 μm (the diffraction limit of the light microscopy) to ~4 μm in length. The $DiIC_{12}$-stained organelles could be detected with a delay of ~10–15 min after the onset of soma labeling. The organelles were transported in an anterograde direction at the rate of 2.93 ± 0.78 μm/s (mean ± SEM of 137 vesicles in 15 neurons), in agreement with previously reported rates of the fast axonal transport (Allen et al., 1982; Nakata et al., 1998). Occasionally, we observed some "hesitation" in this anterograde transport; however, none of the organelles changed direction of movement (total of 1,578 vesicles in 26 neurons; average observation distance ~150 μm). This result suggests that the polarity of axonal MTs in growing *Xenopus* neurites is uniform. Staining of neuronal cultures with rhodamine-123, a mitochondria-specific fluorescent dye, indicated that the movement of mitochondria from the soma to the axon was a very rare event. The majority of mitochondria frequently changed their direction of movement and did not translocate over long distances along the axon (data not shown). Moreover, $DiIC_{12}$-stained tubovesicular organelles were able to fuse with the plasmalemma (see below). Accordingly, we conclude that the overwhelming majority of $DiIC_{12}$-stained vesicles detected along the axon are distinct from mitochondria.

No fluorescent vesicles could be detected at the distal axon within 1 h after the labeling of the cell body if the longer hydrocarbon chain $DiIC_{12}$ analogue, $DiIC_{18}$, was used. These data are consistent with the scenario in which the lypophilic long-chain $DiIC_{18}$ molecules are restricted to the plasma membrane. Because of the low level of constitutive endocytic activity at the soma region (Bunge, 1977), the rate of internalization of $DiIC_{18}$ molecules is low. Therefore, the appearance of $DiIC_{12}$-labeled vesicles at the distal axon reflected a redistribution of $DiIC_{12}$ molecules from the plasma membrane to the cytoplasm, and nonspecific staining of all lipid-containing organelles in the cell body. These organelles were transported anterogradely, and at sufficiently large distances from the soma, they could be visualized in the absence of plasma membrane staining.

Cell Body–derived Vesicles Are Transported to the Growth Cone Region and Fuse with the Plasma Membrane

Within 10–20 min after the staining of the cell body, we observed an accumulation of $DiIC_{12}$-labeled vesicles at the

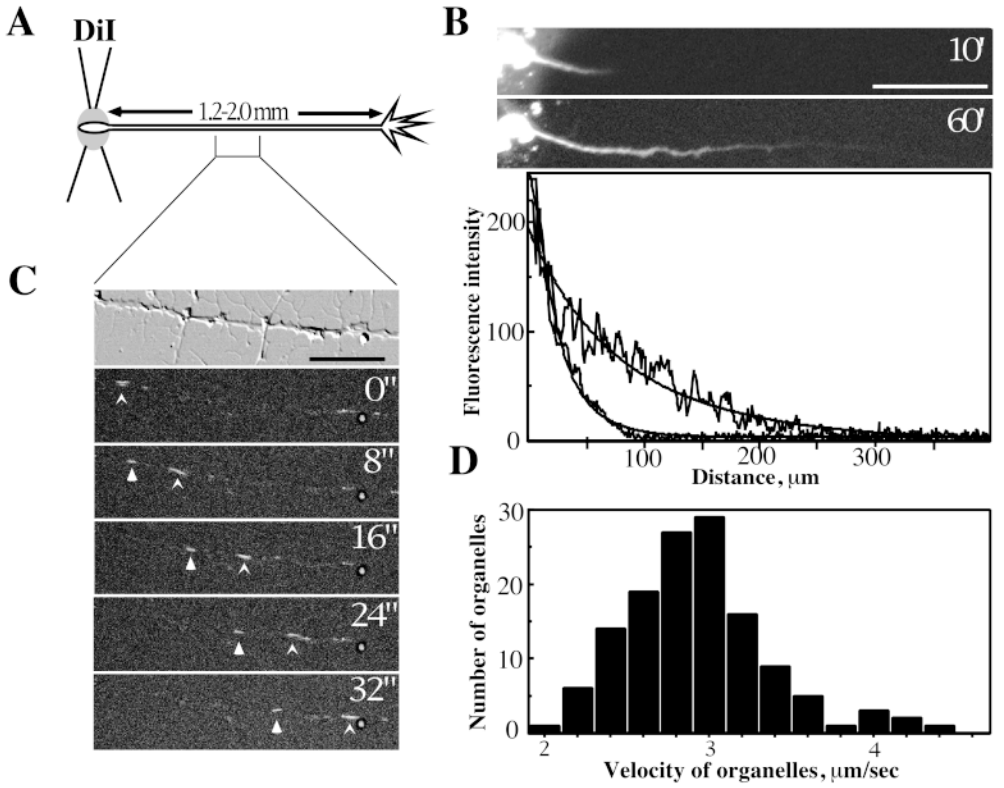

Figure 1. Staining of cell body–derived vesicles with the fluorescent lipid analogue $DiIC_{12}$. (*A*) Schematic representation of experimental approach. The cell body of a neuron was locally labeled with $DiIC_{12}$ molecules using a pair of perfusion pipettes. One pipette was used for the delivery of $DiIC_{12}$-containing solution to the soma region, and another for its removal. The pipettes were withdrawn from the soma 30–60 s after the onset of perfusion. (*B*) Fluorescence images of the soma and the proximal axon at two different times (marked in minutes) after $DiIC_{12}$ incorporation into the plasmalemma, and corresponding profiles of fluorescence intensities (arbitrary units) along the axon. (*C*) Differential interference contrast (*top*) and fluorescence images of the axonal segment located 0.7 mm from the cell body 15 min after local labeling of the soma. No plasma membrane staining could be detected. The arrows track two rapidly moving fluorescent organelles (time in seconds). (*D*) The distribution of velocities of the $DiIC_{12}$-labeled organelles. 137 organelles were chosen randomly. Measurements of the rates of organelle movement were made by determining the displacement of the vesicles for a period of 60 s. All vesicles moved anterogradely. Bars: (*B*) 100 μm; (*C*) 25 μm.

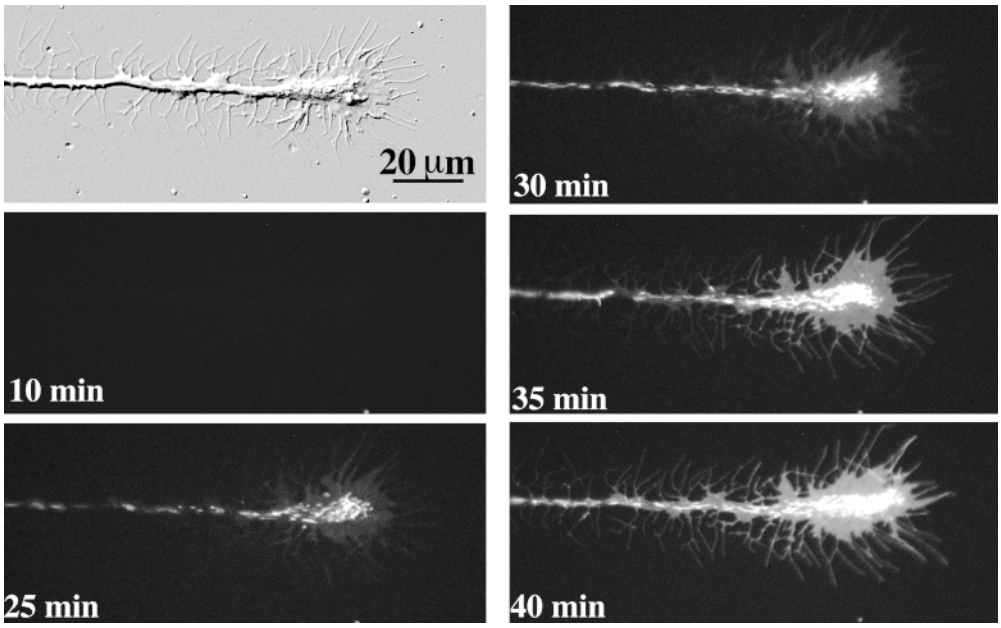

Figure 2. Progressive staining of the distal axon after labeling of cell body–derived vesicles. DIC and fluorescence images of the distal axon at different times (marked in minutes) after local labeling of cell body–derived vesicles with $DiIC_{12}$ molecules. The length of the axon was ~1,900 μm. $DiIC_{12}$-labeled vesicles gradually accumulated at the central domain of the growth cone. The delay between the staining of the cell body and accumulation of the vesicles at the distal axon is likely to reflect the time required for the fast axonal transport of the vesicles. Notice a gradual increase in the diffuse staining of the vesicle-free peripheral growth cone.

central cytoplasmic domain of the growth cone (Fig. 2). Individual vesicles could be resolved as brightly stained puncta both along the axon (Fig. 1) and at the growth cone region (Figs. 2 and 3). In parallel with accumulation of $DiIC_{12}$-labeled vesicles at the distal axon, we observed a progressive increase in the diffuse staining of the peripheral growth cone region (Fig. 2). In agreement with previously published data (Forscher and Smith, 1988), the cell body–derived vesicles were largely excluded from the peripheral growth cone lamella and from the filopodia (Figs. 2 and 3). Therefore, we interpret the diffuse staining of the axon as incorporation of $DiIC_{12}$ molecules into the plasma membrane. This diffuse staining gradually spread from the growth cone towards the cell body (Fig. 2), consistent with lateral diffusion of $DiIC_{12}$ molecules along the plasmalemma.

Since no plasma membrane staining at the middle axonal segment could be detected (Fig. 4 *A*), the staining of the peripheral growth cone was not due to the diffusion of $DiIC_{12}$ molecules from the soma along the plasmalemma. Hence, the diffuse staining of the growth cone reflected the fusion of $DiIC_{12}$-labeled vesicles with the plasma membrane at the distal axon. To test this model, before the staining of the soma with $DiIC_{12}$, we pretreated neuronal cultures for 1 h with brefeldin A (10 μg/ml), a drug that inhibits the supply of the new membrane to the axon (Lippincott-Schwartz et al., 1989; Jareb and Banker, 1997). As expected, the number of $DiIC_{12}$-labeled vesicles at the dis-

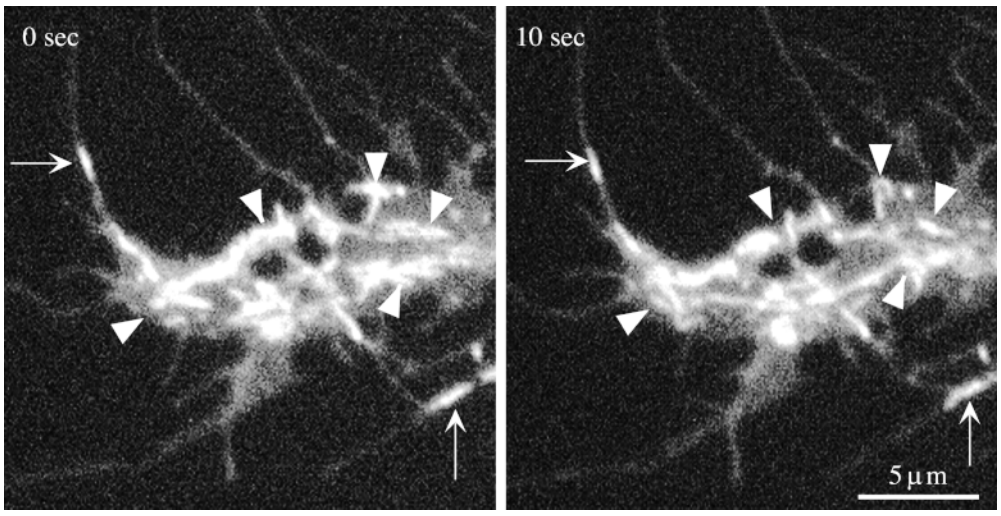

Figure 3. Individual $DiIC_{12}$-labeled vesicles at the growth cone region. Two fluorescence images (time in seconds) of the growth cone region taken ~20 min after the labeling of cell body–derived vesicles with $DiIC_{12}$ molecules. Individual $DiIC_{12}$-labeled vesicles are detected as bright puncta. Vesicles (*arrowheads*) are able to move within the growth cone. Although occasionally $DiIC_{12}$-labeled vesicles could be found in the filopodia (*arrows*), most of the vesicles were excluded from the filopodia. Note uniform diffuse staining of the vesicle-free filopodia and flat lamellipodium-like protrusions. Since individual vesicles are excluded from these structures, the diffuse staining is likely to reflect the incorporation of $DiIC_{12}$ molecules into the plasmalemma.

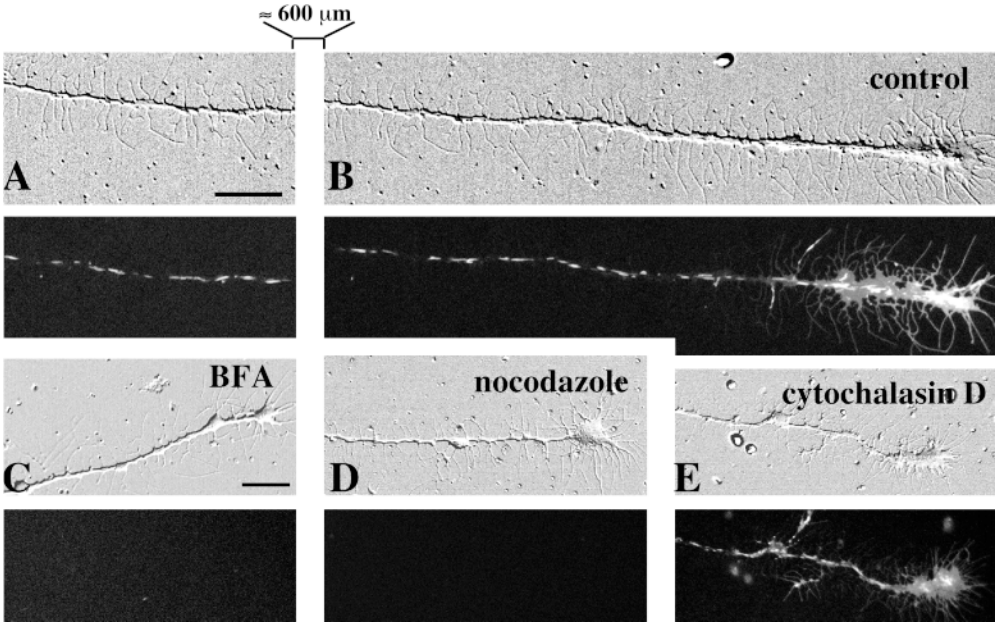

Figure 4. Preferential insertion of cell body–derived vesicles into the growth cone region. (*A* and *B*) DIC (*top*) and fluorescence (*bottom*) images of the middle (*A*) and distal (*B*) segments of the same axon 30 min after staining of the cell body. The length of the axon was ~1,600 μm, and the middle segment was ~900 μm away from the soma. Staining of the plasma membrane with $DiIC_{12}$ molecules, reflecting the insertion of $DiIC_{12}$-labeled vesicles into the plasmalemma, could be observed at the growth cone (*B*). No plasma membrane staining was detected at the middle axon, as well as at sufficiently large distances from the growth cone in the distal segment (*A* and *B*). (*C–E*) Differential interference contrast and fluorescent micrographs of the distal axons 60 min after the staining of the cell body. Before the staining of the soma, neuronal cultures were pretreated for 1 h with brefeldin A (10 μg/ml, *C*), nocodazole (5 μg/ml, *D*), or cytochalasin D (5 μM, *E*). The drugs were present in the culture medium throughout the experiment. Very few (*C*) or no (*D*) fluorescent vesicles and no plasma membrane staining (*C* and *D*) could be detected. Cytochalasin treatment (*E*) had no obvious effect on the delivery of the vesicles to the growth cone and their incorporation into the plasma membrane. Bars, 30 μm.

tal axon was dramatically reduced, and no plasma membrane staining could be detected (Fig. 4 *C*). No fluorescent vesicles could be detected at the distal axon after the treatment of neuronal cultures with 5 μg/ml nocodazole, a drug that promotes MT disassembly (Fig. 4 *D*). This is consistent with the idea that the transport of the cell body–derived vesicles from the soma crucially depends on the integrity of axonal MTs. Cytochalasin D (5 μM), a drug that inhibits actin polymerization, had no obvious effect on organelle delivery to, and incorporation into, the distal axon (Fig. 4 *E*). Similar results were obtained with latrunculin A (5 μM), a drug that induces depolymerization of actin filaments (data not shown). To investigate whether the drugs used in this study induced significant disassembly or assembly of axonal MTs, we loaded fluorescently labeled tubulin into neurons by embryo injection (Reinch et al., 1991; Chang et al., 1998) and examined the neurons with fluorescent microscopy. Detergent extraction of the neurons in an MT-stabilizing buffer revealed that 76.6 ± 4.4% (mean ± SEM, data from 15 axons) of the total tubulin was in the polymer form. 1 h after the treatment of neuronal cultures with brefeldin A (10 μg/ml) or with cytochalasin D (5 μM), this value was not significantly different from control (Table I). On the contrary, 1 h after the treatment with nocodazole (5 μg/ml), the fraction of the tubulin in polymer form decreased to ~11% (Table I).

Taken together, these results suggest that, in growing axons, the newly synthesized plasma membrane components are transported in the form of tubovesicular organelles along axonal microtubules. The new membrane material is delivered to the growth cone region where it is inserted into the plasmalemma.

Inhibition of Dynamic Instability of Axonal Microtubules Prevents Insertion of New Membrane at the Growth Cone Region

MTs at the growth cone region display a complex pattern of behavior and appear to be significantly more dynamic than MTs along the axon (Bamburg et al., 1986; Tanaka and Kirschner, 1991; Tanaka et al., 1995). To test whether the high rate of MT turnover at the distal axon contributes to the preferential insertion of the cell body–derived vesicles at the growth cone region, we determined the effects

Table I. Effect of Pharmacological Treatments on the Total Mass of Polymerized Tubulin in Xenopus Embryo Neurons

Drug	Fluorescence intensity
Control	76.6 ± 4.4 (16)
Taxol (7 nM)	75.2 ± 13.4 (6)
Vinblastine (3 nM)	73.5 ± 8.7 (7)
Brefeldin A (10 μg/ml)	68.4 ± 7.1 (9)
Cytochalasin D (5 μM)	71.5 ± 6.2 (12)
Nocodazole (5 μg/ml)	10.8 ± 2.8 (7)*
Vinblastine (1 μM)	14.1 ± 2.0 (9)*

Xenopus embryos were injected with Cy3-tubulin at the two-cell stage, allowed to develop to stages 19–24, and were then used for the preparation of neuronal cultures. The cultures were treated with various drugs for 1 h. Neurons containing fluorescently labeled tubulin were extracted in a MT-stabilizing buffer (see Materials and Methods). For each axon, the fluorescence intensity after extraction was normalized to that before extraction. The data are presented as a mean ± SEM for 6–15 different neurons. *$P < 0.001$, *t* test. In a series of control experiments, the neurons were loaded with FITC-conjugated dextran (mol wt 70,000) and extracted in an MT-stabilizing buffer. The average ratio of the fluorescence intensity after extraction to that before extraction was 3.0 ± 0.6% (data from seven different neurons), suggesting almost complete washout of cytosolic molecules during extraction.

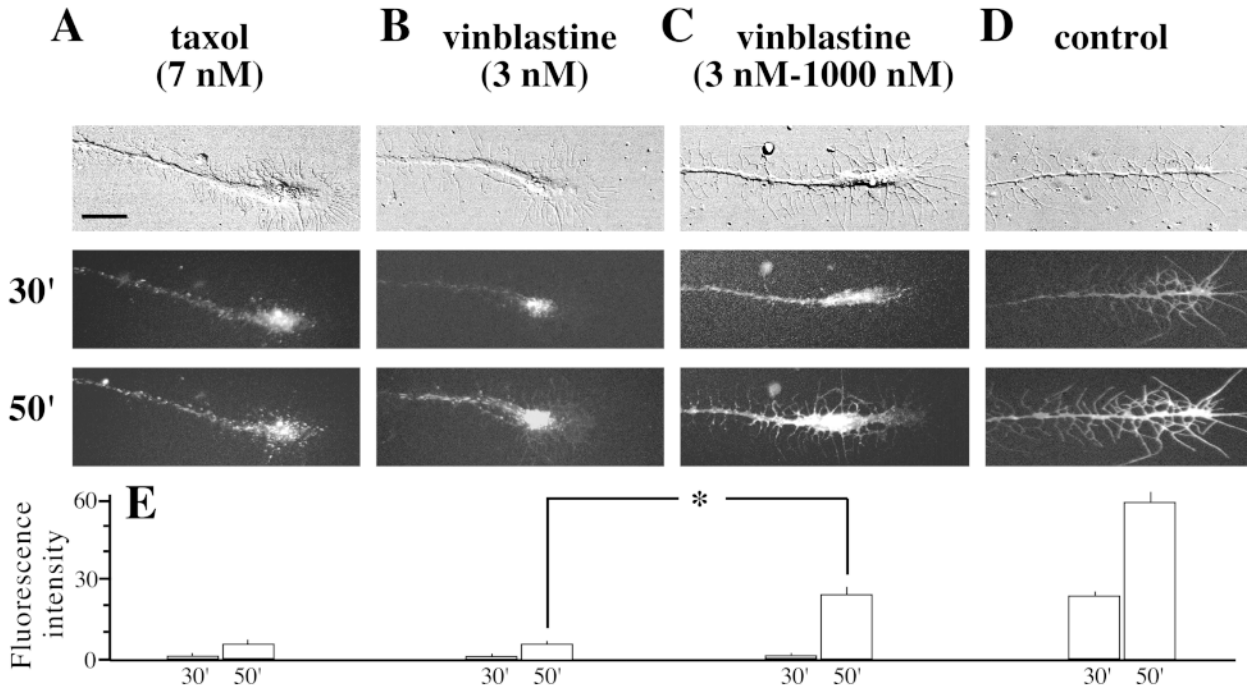

Figure 5. Dynamic instability of MTs is required for the insertion of new membrane into the distal axon. (*A–D*) DIC (*top*) and fluorescence images of the distal axon at two different times (marked in minutes) after the staining of the soma. 7 nM taxol (*A*) or 3 nM vinblastine (*B* and *C*) was added to the culture medium 30 min before the staining of the soma. Fluorescent vesicles accumulated at the growth cone region. Filopodia staining in *A* and *B* was drastically reduced in comparison with control (*D*) neurons ($P < 0.001$, *t* test). In *C*, 30 min after the staining of the cell body, the concentration of vinblastine was increased to 1 μM. This induced a rapid insertion of the vesicles accumulated at the distal axon into the plasma membrane and staining of the filopodia. (*E*) Quantitative analysis of the plasma membrane staining. For each neuron the intensity of the plasma membrane staining at the growth cone region was determined as an average for at least 20 filopodia. The data are presented as a mean ± SEM for five to seven different neurons. *$P < 0.001$, *t* test. Bar, 30 μm.

of low concentrations of taxol and vinblastine on the pattern of membrane insertion into the growing axons. Taxol and vinblastine are antimitotic drugs that, in micromolar concentrations, stabilize and disrupt MTs, respectively. In nanomolar concentrations, both drugs decrease the dynamic instability of MTs (Jordan et al., 1992, 1993). In nanomolar concentrations, vinblastine and taxol did not affect the polymerization of MTs in *Xenopus* neurons (Table I). Neither taxol (7 nM) nor vinblastine (3 nM) affected the delivery of cell body–derived vesicles to the distal axon, as evidenced by the accumulation of the $DiIC_{12}$-stained organelles at the growth cone region (Fig. 5, *A* and *B*). However, the staining of the plasma membrane, and thus insertion of new membrane into the growth cone region, were dramatically inhibited. The quantitative analysis of the plasma membrane staining (Fig. 5 *E*) was facilitated by the fact that under the cell culture conditions used in this study, axons possess a rich net of filopodia that spans the entire length of the neurite, including the growth cone. Since $DiIC_{12}$-labeled vesicles were largely excluded from the filopodia, the sampling areas were chosen along the length of individual filopodia at the growth cone. Similar results were obtained when the sampling areas were chosen at the lamellipodium region of the growth cone. In a series of control experiments, neuronal cultures were pretreated with 3 nM vinblastine for 30 min to allow accumulation of the fluorescent vesicles at the growth cone region, after which the concentration of vinblastine was increased to 1 μM. This treatment resulted in the disassembly of axonal MTs (data not shown), and rapid staining of the plasma membrane at the distal axon (Fig. 5 *C*). Hence, inhibition of membrane insertion by nanomolar concentrations of vinblastine is not related to a nonspecific effect of the drug on vesicular fusion.

Local Disassembly of Axonal Microtubules Leads to Insertion of Cell Body–derived Vesicles into the Plasma Membrane along the Axon

Under the cell culture conditions used in this study, the majority of $DiIC_{12}$-stained vesicles are transported all the way down to the growth cone region, where the vesicles fuse with the plasma membrane. The insertion of cell body–derived vesicles along the axon may be inhibited because of the limitations imposed by the axonal cytoskeleton. Alternatively, the plasma membrane along the axon may lack the appropriate membrane receptors (t-SNAREs), which are necessary for vesicular targeting and/or fusion (Rothman, 1994; Calacos and Scheller, 1996; Hanson et al., 1997). To distinguish between these possibilities, we locally applied nocodazole (5 μg/ml) to the middle axonal segment located at least ~500 μm away

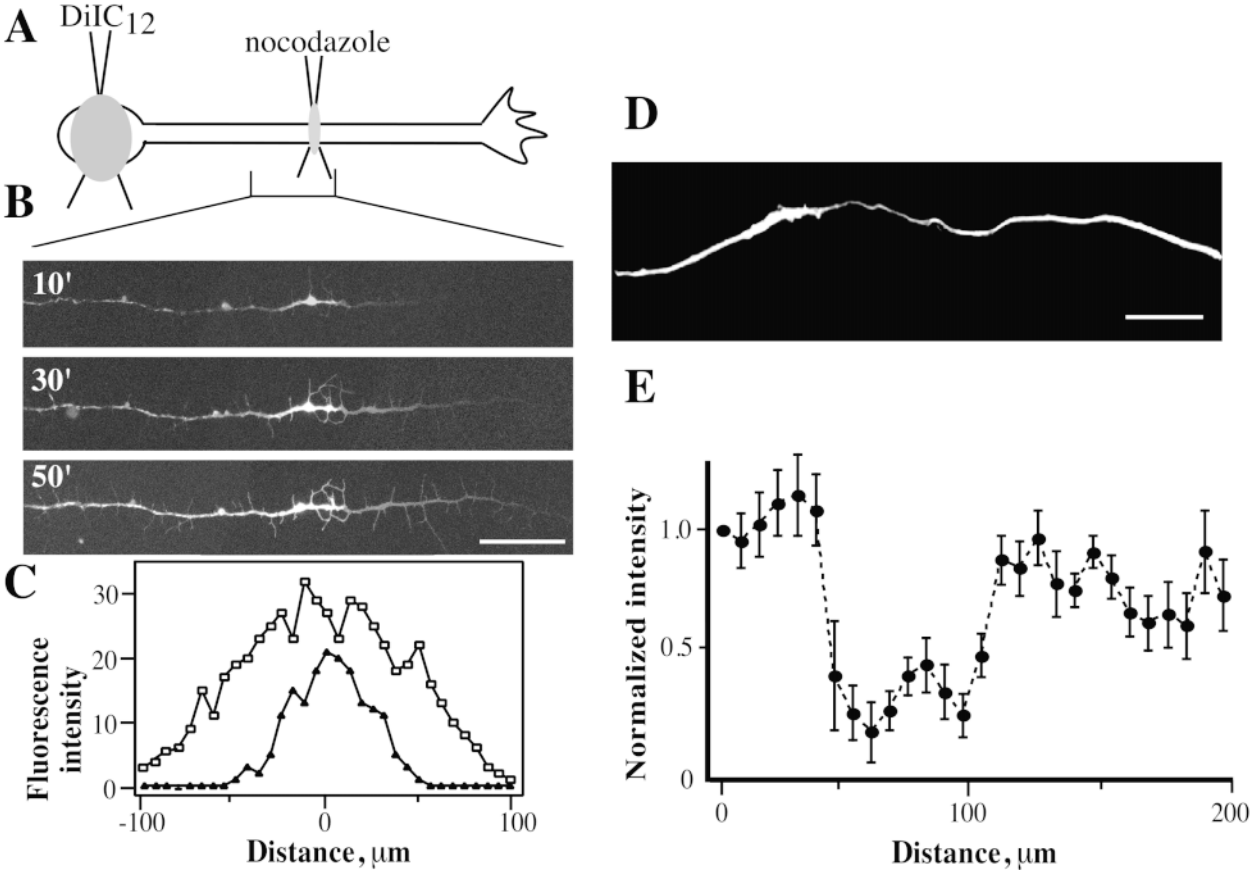

Figure 6. Local disruption of axonal MTs is sufficient for the insertion of cell body–derived vesicles along the axon. (*A*) Cell body–derived vesicles were stained with $DiIC_{12}$ molecules as in Fig. 1. Local perfusion of the middle axonal segment with a culture medium containing 5 μg/ml nocodazole was started 30 min before the soma staining. (*B*) Fluorescent images of the superfused site at different times (marked in minutes) after the staining of the cell body with $DiIC_{12}$. The staining of filopodia, which reflects the insertion of soma-derived vesicles into the plasmalemma, could be detected as soon as 10 min after the onset of cell body staining. The bright staining of the axon proximal to the perfusion site reflects an accumulation of fluorescent vesicles in this region. (*C*) Fluorescence intensity profiles of the filopodia staining 10 min (*filled triangles*) and 50 min (*open squares*) after the soma staining. The intensity of individual filopodia staining (arbitrary units) is plotted vs. the distance from the center of the profile. The center of the superfused zone was located ~50 μm distal from the center of the fluorescence profile. The widening of the profiles reflects the lateral diffusion of $DiIC_{12}$ molecules incorporated into the plasma membrane along the axon. Data from three representative experiments are combined together. (*D*) Representative immunofluorescent micrograph of the MT array in the axon near the site locally superfused with nocodazole. The cell was fixed and stained for MTs 30 min after the onset of perfusion. (*E*) Quantitative analysis of immunofluorescence data. For each axon, the intensity of fluorescence along the axon was normalized to that ~100 μm proximal to the center of the superfused zone. Data are presented as mean ± SEM for 10 different axons. Bars: (*B*) 50 μm; (*D*) 30 μm.

both from the soma and the growth cone. This distance was sufficient to exclude the lateral diffusion of $DiIC_{12}$ molecules from the soma or the growth cone region to the superfused site. 30 min after the onset of perfusion with nocodazole, we stained cell body–derived vesicles with $DiIC_{12}$ molecules as described above. Within 10–20 min after the staining of the soma, we observed the accumulation of cell body–derived organelles 50–80 μm proximal to the perfusion site, local staining of the plasma membrane, and depolymerization of MTs at the perfusion site (Fig. 6). Thus, plasma membrane components for vesicular exocytosis are likely to be present throughout the whole axonal surface. Local disruption of MTs along the axon is sufficient to induce the fusion of cell body–derived vesicles with the plasma membrane.

Discussion

New membrane components are synthesized in the cell body and conveyed along MTs by the kinesin superfamily of proteins (Brady and Sperry, 1995; Block, 1998; Hirokawa, 1998). To determine the sites of new membrane insertion into the growing neurites, we developed a technique for the acute labeling of all membrane structures in the cell body with the fluorescent lipid analogue $DiIC_{12}$. In sufficiently long neurites, we were able to visualize the anterograde transport of individual cell body–derived tubovesicular organelles. The movement of these organelles occurred at the rates of fast axonal transport and required the integrity of axonal MTs. The number of the stained vesicles along the axon was dramatically diminished after pretreatment of neuronal cultures with brefel-

din A. These results along with previously reported data (Nakata et al., 1998) suggest that the cell body–derived tubovesicular organelles that we observe are likely to be involved in the constitutive delivery of newly synthesized membrane material from the Golgi complex to the plasma membrane. There are three major findings in this report: (*a*) under cell culture conditions used in this study, the vesicles were delivered all the way down to the growth cone region, where they fused with the plasma membrane; (*b*) local disruption of MTs at the middle axonal segment resulted in the insertion of new membrane along the axon; and (*c*) inhibition of dynamic instability of axonal microtubules impaired the insertion of new membrane material into the distal axon.

Preferential insertion of some of the newly synthesized plasma membrane proteins into the growth cone region has been observed in the past (Craig et al., 1995; Vogt et al., 1996). Our results provide direct evidence for the idea that the growth cone is the primary site of new membrane addition to the plasmalemma (Futerman and Banker, 1996). Exocytosis of $DiIC_{12}$-stained vesicles along the axon would be expected to result in the disappearance of the fluorescent signal because of the rapid diffusion of $DiIC_{12}$ molecules along axonal plasmalemma. We were not able to detect such fusion events. Although we cannot exclude the possibility that some of the small vesicles escape detection and do fuse with the plasmalemma along the axon, the vast majority of the vesicles appeared to be transported all the way down to the growth cone. This conclusion was further supported by the staining of the plasma membrane at the growth cone region, but not at the middle axon (Fig. 4). Interestingly, the staining of the plasma membrane at the distal axon was preceded by an accumulation of $DiIC_{12}$-labeled vesicles at this region. The observed delay in the insertion of new membrane into the plasmalemma is consistent with the idea that a number of intermediate steps (such as vesicular docking and priming) are required for the exocytotic fusion to proceed (Sudhof, 1995). It should be noted that only cell body–derived vesicles were stained in our experiments. We have not attempted to determine the contribution of local synthesis of plasma membrane lipids along the neurite (de Chaves et al., 1995) to the generation of new axonal structure.

Although the idea of preferential insertion of new membrane components into the distal axon is now widely accepted, a simple estimate based on the diffusion equation indicates that in sufficiently long axons, new membrane is likely to be inserted along the axon. Indeed, the coefficient of lateral diffusion of the plasma membrane proteins or lipids (D) does not exceed 10^{-8} cm^2/s (Tank et al., 1982). Assuming that the newly synthesized membrane material is inserted exclusively into the growth cone region, the characteristic time of diffusional transport from the growth cone region (t) can be estimated as $t \approx L^2/D$, where L is the distance from the growth cone. Even for relatively short distances ($L = 1$ mm), this time is ~10 d. Thus, in the absence of anterograde (Popov et al., 1993) or retrograde (Dai and Sheetz, 1995) plasma membrane flow, intercalation of plasma membrane proteins and lipids along the axon is the only feasible mechanism for new material delivery to the axonal shaft (Bloom and Goldstein, 1998). Rigorous quantitative analysis supports the idea that, in sufficiently long axons, axonal plasma membrane components should be inserted at sites all along the axon (Khanin et al., 1998).

This model predicts that the molecular components that are required for vesicular exocytosis are distributed throughout the whole axonal surface. In agreement with this prediction, in hippocampal cultures, both immunocytochemical data (Galli et al., 1995; Garcia et al., 1995) and reports on the constitutive membrane recycling along the axon (Matteoli et al., 1992) imply the presence of t-SNAREs throughout the whole axonal surface. In *Xenopus* embryo neurons, constitutive secretion of acetylcholine can be detected throughout the whole neuronal surface; moreover, similar to hippocampal cultures, immunoreactivity for syntaxin and SNAP-25 can be detected along the axon (Antonov et al., 1998). Taken collectively, these results suggest that axonal shaft is competent to support vesicular exocytosis. Our experiments with local application of nocodazole to the middle axon directly confirm this idea. We found that local disruption of axonal MTs led to the accumulation of cell body–derived vesicles at the site of nocodazole application and insertion of the vesicles into the plasmalemma (Fig. 6). Thus, local disruption of axonal MTs is sufficient for the insertion of new membrane material to specific neuronal sites.

These experiments suggest a mechanistically simple model in which association of a vesicle with an MT limits its access to the plasma membrane. The movement of individual vesicles along MTs is driven by the members of kinesin superfamily of proteins (Vale et al., 1996; Block, 1998; Hirokawa, 1998). Kinesin remains bound to MTs while undergoing multiple rounds of activity (Vale et al., 1996; Block, 1998). The average distance traveled by a single kinesin molecule after a binding to an MT is about 600 nm in a motility assay (Vale et al., 1996). Obviously, if the movement of the vesicle is driven by more than one kinesin molecule associated with the same MT, the average travel distance along the MT will be larger. However, MTs are much shorter than axonal length, and the vesicle is expected to "fall off" the MT upon reaching its plus (directed towards the growth cone) end. We speculate that because of the high density of MTs in the axonal shaft, the dissociated vesicle is likely to reattach rapidly to another (or to the same) MT. Therefore, the probability of vesicular exocytosis along the axon remains low.

It remains to be established what properties of the growth cone region allow exocytosis to proceed. Since none of cell body–derived vesicles that we detected was transported retrogradely, the vesicles are expected to accumulate at the distal axon. Unique molecular composition of the growth cone region may contribute to trapping of the vesicles in the cytomatrix and/or facilitate their translocation to the plasma membrane. Unexpectedly, we found that inhibition of dynamic instability of MTs dramatically impaired insertion of new membrane into the distal axon. The easiest interpretation of these data is that dynamic instability of MTs at the growth cone region increases the probability of dissociation of a vesicle from an MT. However, we cannot exclude the possibility that dynamic MTs at the distal axon are essential for the proper organization of the apparatus for the delivery of the vesicles to the plasma membrane sites specialized for fusion.

Treatment of neuronal cultures with low doses of vinblastine or taxol is known to inhibit axonal elongation (Tanaka et al., 1995) and growth cone turning (Challacombe et al., 1997). These results are believed to reflect the essential role of dynamic MTs in the rearrangement of MTs during growth cone migration and in the generation of new axonal structure (Tanaka et al., 1995; Challacombe et al., 1997). Our results suggest that dynamic instability of microtubules at the distal axon may also contribute to the release of vesicles from the MTs and insertion of new membrane into the growth cone region. Therefore, the effect of low doses of taxol and vinblastine on growth cone migration, at least in part, may be related to the inhibition of new membrane addition to the plasmalemma.

Tubulin dimers must contain GTP to polymerize. GTP is rapidly hydrolyzed upon addition of dimers to the growing MT. This creates a small cap of GTP-tubulin at the growing end of an MT, while MT lattice is primarily composed of GDP-tubulin (Desai and Mitchison, 1997). Both kinetochores (Inoue and Salmon, 1995; Severin et al., 1997) and membrane organelles (Blocker and Griffiths, 1998) recognize MT plus ends (presumably through their association with GTP cap), and their movement can be powered by MT dynamics (Desai and Mitchison, 1995; Lombillo et al., 1995). Therefore, dynamic changes in MT length may directly contribute to intracellular motility (Desai and Mitchison, 1995; Inoue and Salmon, 1995). Moreover, experimental evidence suggests that motors may not easily detach from MTs when they reach their ends (Verde et al., 1991; Hyman and Karsenti, 1996). Our data suggest that dynamic instability of axonal MTs can increase the probability of vesicle dissociation from the MT and regulate the number of cell body–derived vesicles available for exocytosis. Thus, dynamics of axonal MTs may serve as a basic regulator of the topology of the new membrane addition to the nerve processes.

We thank Gary Borisy, Vladimir Gelfand, Leonid Margolis, and Mark Rasenick for the helpful discussion and comments and Michael O'Donoghue for help with the manuscript. We are grateful to Regeneron Pharmaceuticals Inc. for providing NT-3 and to Gary Borisy for providing Cy3-tubulin.

Supported by The National Institutes of Health (NS 33570).

Received for publication 16 July 1998 and in revised form 30 September 1998.

References

Abercrombie, M., J.E.M. Heaysman, and S.M. Pengrum. 1970. The locomotion of fibroblasts in culture. III. Movement of particles on the dorsal surfaces of the leading lamella. *Exp. Cell Res.* 62:389–398.

Allen, R.D.J., J. Metuzals, S.T. Tasaki, S.T. Brady, and S.P. Gilbert. 1982. Fast axonal transport in squid giant axon. *Science.* 218:1127–1129.

Anderson, M.J., M.W. Cohen, and E. Zorychta. 1977. Effects of innervation on the distribution of acetylcholine receptors on cultured muscle cells. *J. Physiol. (Lond.).* 268:731–758.

Antonov, I., S. Chang, S. Zakharenko, and S. Popov. 1998. Topology of exocytotic events in growing axons. *Neuroscience.* In press.

Bamburg, J.R., D. Bray, and K. Chapman. 1986. Assembly of microtubules at the tip of growing axons. *Nature.* 321:788–790.

Block, S.M. 1998. Leading the procession: new insights into kinesin motors. *J. Cell Biol.* 140:2181–2184.

Blocker, A., and G. Griffiths. 1998. A role for microtubule dynamics in phagosome movement. *J. Cell Sci.* 111:303–312.

Bloom, G.S., and L.S.B. Goldstein. 1998. Cruising along microtubule highways: how membranes move through the secretory pathway. *J. Cell Biol.* 140:1277–1280.

Brady, S.T., and A.O. Sperry. 1995. Biochemical and functional diversity of microtubule motors in the nervous system. *Curr. Opin. Neurobiol.* 5:551–558.

Bray, D. 1970. Surface movements during the growth of single explanted neurons. *Proc. Natl. Acad. Sci. USA.* 65:905–910.

Bunge, M.B. 1977. Initial endocytosis of peroxidase of ferritin by growth cones of cultured nerve cells. *J. Neurocytol.* 6:407–439.

Calacos, N., and R. Scheller. 1996. Synaptic vesicle biogenesis, docking and fusion: a molecular description. *Physiol. Rev.* 76:1–29.

Challacombe, J.F., D.M. Snow, and P.C. Letourneau. 1997. Dynamic microtubule ends are required for growth cone turning to avoid an inhibitory guidance cue. *J. Neurosci.* 17:3085–3095.

Chang, S., V.I. Rodionov, G.G. Borisy, and S.V. Popov. 1998. Transport and turnover of microtubules in frog neurons depend on the pattern of axonal growth. *J. Neurosci.* 18:821–829.

Craig, A.M., and G. Banker. 1994. Neuronal polarity. *Annu. Rev. Neurosci.* 17: 267–310.

Craig, A.M., R.J. Wyborski, and G. Banker. 1995. Preferential addition of newly synthesized membrane protein at axonal growth cones. *Nature.* 375: 592–594.

Dai, D.J., and M.P. Sheetz. 1995. Axon membrane flows from the growth cone to the cell body. *Cell.* 83:693–701.

de Chaves, E.P., D.E. Vance, R.B. Campenot, and J.E. Vance. 1995. Axonal synthesis of phosphatidylcholine is required for normal axonal growth in rat sympathetic neurons. *J. Cell Biol.* 128:913–918.

Desai, A., and T.J. Mitchison. 1995. A new role for motor proteins as couplers to depolymerizing microtubules. *J. Cell Biol.* 128:1–4.

Desai, A., and T.J. Mitchison. 1997. Microtubule polymerization dynamics. *Annu. Rev. Cell Dev. Biol.* 13:83–117.

Engert, F., and T. Bonhoeffer. 1997. Synapse specificity of long-term potentiation breaks down at short distances. *Nature.* 388:279–284.

Feldman, E.L., D. Axelrod, M. Schwartz, A.M. Heacock, and B.W. Agranoff. 1981. Studies of the localization of newly added membrane to growing neurites. *J. Neurobiol.* 12:591–598.

Forscher, P., and S.J. Smith. 1988. Actions of cytochalasins on the organization of actin filaments and microtubules in a neuronal growth cone. *J. Cell Biol.* 107:1505–1516.

Futerman, A.H., and G.A. Banker. 1996. The economics of neurite outgrowth—the addition of new membrane to growing axons. *Trends Neurosci.* 19:144–149.

Galli, T., E.P. Garcia, O. Mundigl, T.J. Chilcote, and P. De Camilli. 1995. v- and t-SNAREs in neuronal exocytosis: a need for additional components to define sites of release. *Neuropharmacology.* 34:1351–1360.

Garcia, E.P., P.S. McPherson, T.J. Chilcote, K. Takei, and P. De Camilli. 1995. rbSec1A and B colocalize with syntaxin 1 and SNAP-25 through the axon, but not in a stable complex with syntaxin. *J. Cell Biol.* 129:105–120.

Griffin, J.W., D.L. Price, D.B. Drachman, and J. Morris. 1981. Incorporation of axolemma during nerve regeneration. *J. Cell Biol.* 88:205–214.

Hanson, P.I., J.E. Heuser, and R. Jahn. 1997. Neurotransmitter release—four years of SNARE complexes. *Curr. Opin. Neurobiol.* 7:310–315.

Harel, R., and A.H. Futerman. 1996. A newly-synthesized GPI-anchored protein, TAG-1/axonin-1, is inserted into axonal membranes along the entire length of the axon and not exclusively at the growth cone. *Brain Res.* 712: 345–348.

Hirokawa, N. 1998. Kinesin and dynein superfamily proteins and the mechanism of organelle transport. *Science.* 279:519–526.

Hyman, A., and E. Karsenti. 1996. Morphogenetic properties of microtubules and mitotic spindle assembly. *Cell.* 84:401–410.

Inoue, S., and E.D. Salmon. 1995. Force generation by microtubule assembly/disassembly in mitosis and related movements. *Mol. Biol. Cell.* 6:1619–1640.

Jareb, M., and G. Banker. 1997. Inhibition of axonal growth by brefeldin A in hippocampal neurons in culture. *J. Neurosci.* 17:8955–8963.

Jordan, M.A., D. Thrower, and L. Wilson. 1992. Effects of vinblastine, podophyllotoxin and nocodazole on mitotic spindles. Implications for the role of microtubule dynamics in mitosis. *J. Cell Sci.* 102:401–416.

Jordan, M.A., R.J. Toso, D. Thrower, and L. Wilson. 1993. Mechanism of mitotic block and inhibition of cell proliferation by taxol at low concentrations. *Proc. Natl. Acad. Sci. USA.* 90:9552–9556.

Khanin, R., L. Segel, and A.H. Futerman. 1998. The diffusion of molecules in axonal plasma membranes: the sites of insertion of new membrane molecules and their distribution along the axon surface. *J. Theor. Biol.* 193:371–382.

Koda, L.Y., and L.M. Partlow. 1976. Membrane marker movement on sympathetic axons in tissue culture. *J. Neurobiol.* 7:157–172.

Lee, J., M. Gustafsson, K.-E. Magnusson, and K. Jacobson. 1990. The direction of membrane lipid flow in locomoting polymorphonuclear leukocytes. *Science.* 247:1229–1233.

Lin, C.H., E.M. Espreafico, M.S. Mooseker, and P. Forscher. 1996. Myosin drives retrograde F-actin flow in neuronal growth cones. *Neuron.* 16:769–782.

Lippincott-Schwartz, J., L. Yuan, J. Bonifacino, and R. Klausner. 1989. Rapid redistribution of Golgi proteins into the ER in cells treated with brefeldin A: evidence for membrane cycling from Golgi to ER. *Cell.* 56:801–813.

Lombillo, V.A., R.J. Stewart, and J.R. McIntosh. 1995. Minus-end-directed motion of kinesin-coated microspheres driven by microtubule depolymerization. *Nature.* 373:161–164.

Martenson, C., K. Stone, M. Reedy, and M. Sheetz. 1993. Fast axonal transport is required for growth cone advance. *Nature.* 366:66–69.

Matteoli, M., K. Takei, M.S. Perin, T.C. Sudhof, and P. De Camilli. 1992. Exo-endocytotic recycling of synaptic vesicles in developing processes of cultured

hippocampal neurons. *J. Cell Biol.* 117:849–861.
Nakata, T., S. Terada, and N. Hirokawa. 1998. Visualization of the dynamics of synaptic vesicle and plasma membrane proteins in living axons. *J. Cell Biol.* 140:659–674.
Okabe, S., and N. Hirokawa. 1992. Differential behavior of photoactivated microtubules in growing axons of mouse and frog neurons. *J. Cell Biol.* 117: 105–120.
Peng, H.B., and P.C. Chang. 1982. Formation of postsynaptic specializations induced by latex beads in cultured muscle cells. *J. Neurosci.* 2:1760–1774.
Pfenninger, K.H., and M.-F. Maylie-Pfenninger. 1981. Lectin labeling of sprouting neurons. II. Relative movement and appearance of glycoconjugates during plasmalemmal expansion. *J. Cell Biol.* 89:547–559.
Popov, S.V., A. Brown, and M.-m. Poo. 1993. Forward plasma membrane flow in growing nerve processes. *Science.* 259:244–246.
Reinch, S.S., T.J. Mitchison, and M.W. Kirschner. 1991. Microtubule polymer assembly and transport during axonal elongation. *J. Cell Biol.* 115:365–379.
Rothman, J.E. 1994. Mechanisms of intracellular protein transport. *Nature.* 372: 55–63.
Severin, F.F., P.K. Sorger, and A.A. Hyman. 1997. Kinetochores distinguish GTP from GDP forms of the microtubule lattice. *Nature.* 388:888–891.
Sheetz, M.P., S. Turney, H. Qian, and E.L. Elson. 1989. Nanometre-level analysis demonstrates that lipid flow does not drive membrane glycoprotein movements. *Nature.* 340:284–289.
Sudhof, T.C. 1995. The synaptic vesicle cycle: a cascade of protein-protein interactions. *Nature.* 375:645–653.
Tanaka, E., and M.W. Kirschner. 1991. Microtubule behavior in the growth cones of living neurons during axon elongation. *J. Cell Biol.* 115:345–363.
Tanaka, E., T. Ho, and M.W. Kirschner. 1995. The role of microtubule dynamics in growth cone motility and axonal growth. *J. Cell Biol.* 128:139–155.
Tank, D.W., E.-S. Wu, and W.W. Webb. 1982. Enhanced molecular diffusibility in muscle membrane blebs: release of lateral constraints. *J. Cell Biol.* 92: 207–212.
Vale, R.D., T. Funatsu, D.W. Pierce, L. Romberg, Y. Harada, and T. Yanagida. 1996. Direct observation of single kinesin molecules moving along microtubules. *Nature.* 380:451–453.
Verde, F., J.-M. Berrez, C. Antony, and E. Karsenti. 1991. Taxol-induced microtubule asters in mitotic extracts of *Xenopus* eggs: requirement for phosphorylated factors and cytoplasmic dynein. *J. Cell Biol.* 112:1177–1187.
Vogt, L., R.J. Giger, U. Ziegler, B. Kunz, A. Buchstaller, W.T. Hermens, M.G. Kaplitt, M.R. Rosenfeld, D.W. Pfaff, J. Verhaagen, and P. Sonderegger. 1996. Continuous renewal of the axonal pathway sensor apparatus by insertion of new sensor molecules into the growth cone membrane. *Curr. Biol.* 6:1153–1158.
Zheng, J., P. Lamoureux, V. Santiago, T. Dennerll, R.E. Buxbaum, and S.R. Heidemann. 1991. Tensile regulation of axonal elongation and initiation. *J. Neurosci.* 11:1117–1125.
Zheng, J.Q., M. Felder, J.A. Connor, and M.-m. Poo. 1994. Turning of nerve growth cones induced by neurotransmitter. *Nature.* 368:140–144.